Simulations of EBW current drive and power deposition in the WEGA Stellarator

J. Preinhaelter[1)], J. Urban[1)], H. P. Laqua[2)], Y. Podoba[2)], L. Vahala[3)], G. Vahala[4)]

1) EURATOM/IPP.CR Association, Institute of Plasma Physics, 182 00 Prague, Czech Republic
2) Max-Plank Institut für Plasmaphysik, EURATOM Ass., D-17491, Greifswald, Germany
3) Old Dominion University, Norfolk, VA 23529, USA
4) College of William & Mary, Williamsburg, VA 23185, USA

Abstract. The WEGA stellarator [1] is well suited for fundamental electron Bernstein wave (EBW) studies. Heating and current drive experiments at 2.45 GHz and 28 GHz, carried out in WEGA's low temperature, steady state overdense plasmas, were supported by intensive modelling. We employ our AMR (Antenna—Mode-conversion—Ray-tracing) code [3] to calculate the O-X-EBW conversion efficiency with a full-wave equation solver, while the power deposition and current drive profiles using ray tracing. Several phenomena have been studied and understood. Particularly, EBW current drive was theoretically predicted and experimentally detected at 2.45 GHz. Simulations confirmed the presence of two (cold and hot) electron components and the resonant behaviour of the EBW power deposition and its dependence on the magnetic field configuration. Furthermore, the code is used to predict the 28 GHz heating and current drive performance and to simulate EBW emission spectra.

Keywords: Stellarator. Electron Bernstein waves.
PACS: 52.55.Fa, 52.35.Hr

Introduction

WEGA is a medium-sized classical $\ell = 2, m = 5$ stellarator, with major radius 72 cm and maximum minor plasma radius 11.5 cm [1]. *In the low magnetic field configuration* ($B_0 = 0.0875$ T), the plasma is generated by up to 26 kW of 2.45 GHz ECRH with a standard steady state discharge of 30 s. The electron density of $\sim 10^{18}$ m^3 makes the plasma overdense for the 2.45 GHz wave. The WEGA plasma, in this case, consists of two components: a cold bulk plasma (with temperatures up to ≈ 10 eV) and a hot component around 300 eV, measured by Langmuir probes [2]. The double-slot antenna has cross section 83 mm and emits a linearly polarized wave with radiation lobes peaked at $\theta = \pm 60^o$. The plasma is underdense in the vicinity of the antenna, which is needed for the O-X-EBW conversion. The 2.45 GHz wave frequency lies between the 1st and 2nd EC harmonics. The maximal O-X-EBW mode conversion efficiency for linearly polarized waves is 60 %. From full wave calculations [3], we find the optimal mode conversion efficiency for the WEGA antenna to be, however, around 15 – 40 %.

Electron Bernstein waves, propagating in a two-component WEGA plasma, are described by the electrostatic dispersion relation where collisions are considered in the

Bhatnagar-Gross-Krook limit. Propagation of short wavelength EBWs in weakly inhomogeneous plasma can be studied using standard ray tracing [4].

The wave damping is accompanied by a toroidal current due to the creation of an asymmetric plasma resistivity [5]. To determine the generated current density we use the formulation of F.R. Hansen et al. [6], but generalized to two component plasma with multiple electron cyclotron resonances:

$$J = -\sum_{\alpha=0}^{1}\sum_{n=0}^{\infty} \frac{e}{m_e v_{Te,\alpha} \nu_\alpha} \frac{3}{2} \left(\frac{v_{res,n}}{v_{Te,\alpha}} \right)^2 \frac{|v_{res,n}|}{v_{res,n}} \frac{4}{5+Z} P_{\mathrm{d},\alpha,n} . \qquad (0.1)$$

Here, the resonant velocity for nth harmonic is $v_{\mathrm{res},n} = (\omega - n\omega_{\mathrm{ce}})/k_{\|}$, $v_{\mathrm{Te},\alpha} = \sqrt{2T_{e,\alpha}/m_{\mathrm{e}}}$ is the electron thermal velocity, ν_α is the collision frequency and α denotes the electron component. To determine the partial power density deposited in the resonant particles $P_{\mathrm{d},\alpha,n}$, we must determine partial damping rates and integrate the power evolution equation for each ray. WEGA discharges are mainly undertaken in single ionized argon. The wave damping in this case is mainly determined by the electron-ion collisions in the cold component but non-elastic collisions of electrons with Ar ions are dominant for the hot electron component.

WEGA can also operate with magnetic fields up to 0.5 T. For such *high field* scenarios, a 28 GHz 8 kW gyrotron is installed for second harmonic heating. X-mode heating is possible if the density is below the cutoff, which is approximately 10^{19} m^{-3}. However, X-mode heating is rather ineffective due to the electron temperature of the order of 100 – 300 eV. With the help of the 2.45 GHz heating (non-resonantly absorbed this time) and possibly the ohmic transformer, it is feasible to increase the density sufficiently to sustain the discharge by 28 GHz O-X-EBW heating [7]. We report here the simulations of this O-X-EBW heating, particularly the coupling properties and power deposition characteristics.

Current drive by 2.45GHz wave

The current density in WEGA was measured by the miniature Rogowski coil and the radial profiles for different B_0 are seen in Fig. 1. The simulations confirmed the negative (opposite to B_0) direction of the current for higher B_0 and also central current reversal for $B_0 = 0.65\, B_{\mathrm{ce}}$. The simulated current is peaked near the region of strong absorption. In the experiment there is time and space averaging and this produces much smoother results. The positive current is caused by the absorption of the power from the left lobe (waves incident

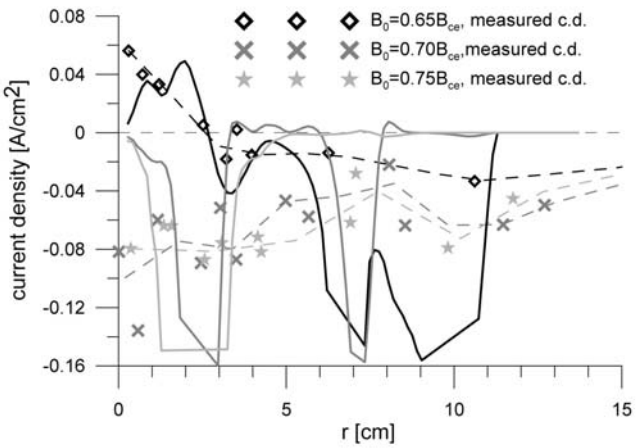

FIGURE 1: B_0 scan of current density radial profiles. Simulations: full black line - $B_0 = 0.65 B_{\mathrm{ce}}$, grey line $B_0 = 0.70 B_{\mathrm{ce}}$, light grey $B_0 = 0.75 B_{\mathrm{ce}}$. Dashed lines are interpolations of corresponding experimental results.

parallel to B_0) near the plasma centre on the second harmonics with $N_{\parallel} > 0$ (see Fig. 2). For higher B_0, the first harmonic absorption dominates producing the negative current density in the centre (see Fig. 3).

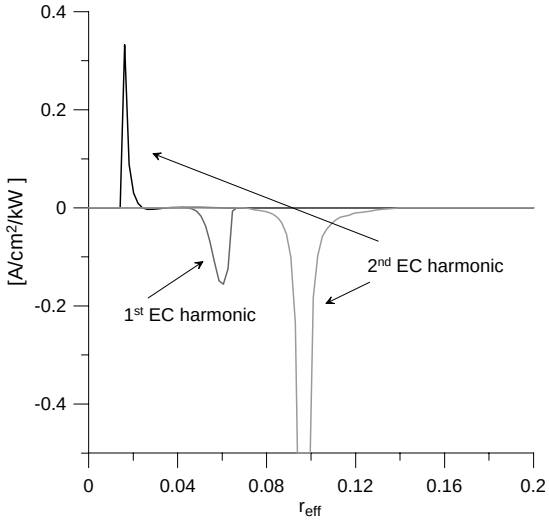

FIGURE 2: Radial profiles of partial contributions to the current density along the central rays of the of two antenna lobes. $B_0 = 0.65 B_{ce}$, $r_{eff} = a_0\sqrt{s}$, where a_0 is the minor radius and s is the magnetic flux label.

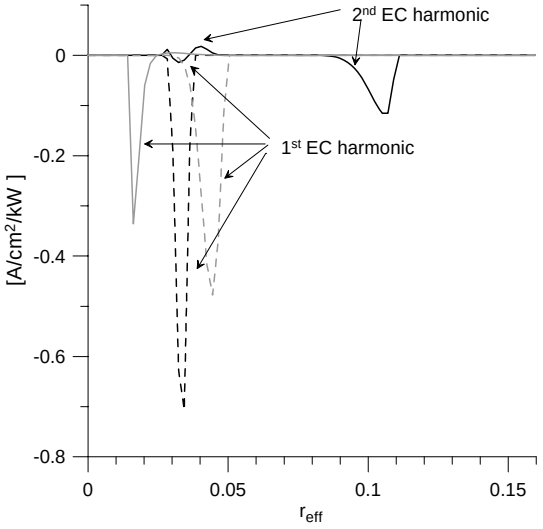

FIGURE 3: Radial profiles of partial contributions to the current density along the central rays of the of two antenna lobes. $B_0 = 0.70 B_{ce}$.

28 GHz O-X-B heating

Experimental data from 28 GHz O-X-EBW discharges have just become available [7]. We present here results from modelling which were performed even before this data was known. Therefore, there is no comparison with the experiment in this paper. Fundamental for the O-X-EBW heating is the coupling efficiency (the transmission window). In the case of 28 GHz, the transmission window is rather wide, as can be seen in Fig. 4. The reasons are the relatively steep density gradient we assume in the simulations ($L_n \cong 2-3\,\mathrm{cm}$) and the reasonably low frequency (long wavelength, $\lambda_{vac} \cong 1\,\mathrm{cm}$). The conversion efficiency then scales approximately as $\exp\left[-L_n/\lambda\left(\Delta N_{\parallel}^2 + \Delta N_{pol}^2\right)\right]$, where ΔN is the deviation from the optimum wave vector component [8].

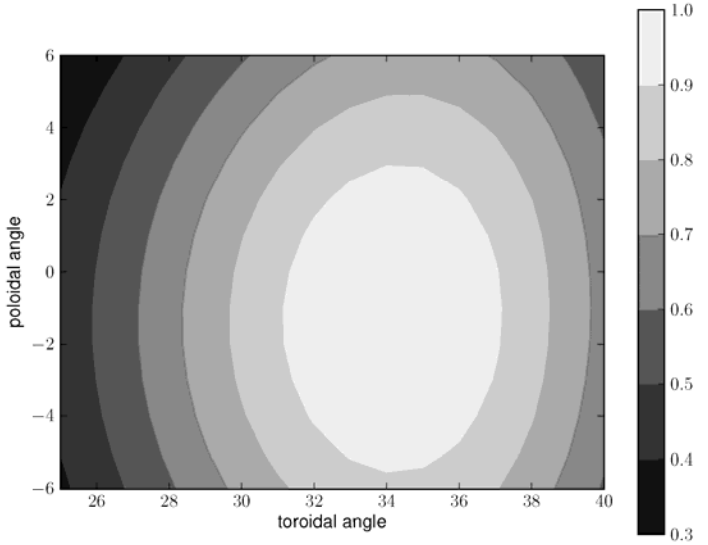

FIGURE 4: Coupling efficiency for the 28 GHz O-X-EBW heating.

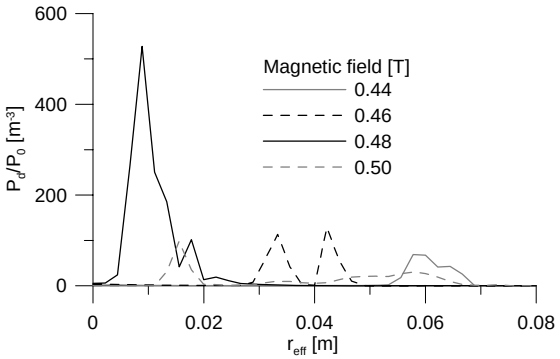

FIGURE 5: Power density of the 28 GHz O-X-EBW heating for various magnetic fields.

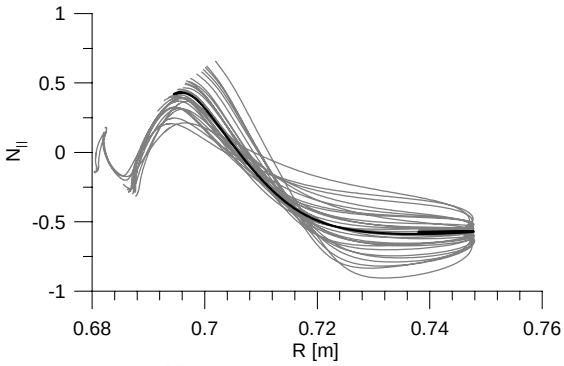

FIGURE 6: $N_{||}$ ray-tracing spectrum of the 28 GHz EBWs, magnetic field 0.48 T.

The magnetic field can be varied and therefore a survey of the deposition profiles with varying magnetic field is carried out. A Gaussian antenna beam placed in the mid-plane and optimally oriented is assumed. The target plasma's peak electron density is 2×10^{19} m^{-3} and the temperature is 350 eV. We note here that the EBW absorption is very efficient even for much lower temperatures and hence the deposition profile is only weakly dependent on the temperature. The magnetic field is varied from 0.44 to 0.5 T by 0.02 T. The resulting power density is plotted in Fig. 5. A sharp peak at 0.48 T is clearly seen in the figure—the most centralized power deposition is observed in this case, making the power density a factor five higher compared to the other cases. The $N_{||}$ ray-tracing spectrum for 0.48 T is plotted in Fig. 6. It is symmetric near the edge, which is to be expected as the beam is launched exactly in the mid-plane. Also expected is the oscillatory behaviour. However, after the first bend, the spectrum becomes asymmetric with $N_{||}$ having the same sign for all the rays. The current has not yet been determined. Moreover, very recently, a suprathermal electron population is observed in the experiments, and this will influence the results in a similar manner to that of the 2.45 GHz case.

Acknowledgments

The work was partly supported by the grant no. 202/08/0419 of Czech Science Foundation, EFDA, U.S. Department of Energy, by EURATOM and by AS CR project AV0Z-20430508.

References

1. Otte M. et. al., 30th EPS Conference on Plasma Phys., St. Petersburg, ECA **27A** (2003) P-1.9.
2. Horvath K. et. al., Plasma Phys. Control. Fusion **48** (2006) 315–323.
3. Urban J. and Preinhaelter J., J. Plasma Phys **72** (2006) 1041-1044.
4. Preinhaelter J., et.al., AIP Conference Proceedings **933** (2007) 343.
5. Fish N. J., Boozer A. H., Phys. Rev. Lett. **45** (1980) 720.
6. Hansen F.R. et. al., PPCF **27** (1985) 1077.
7. Laqua H.P. et al., these proceedings.
8. Preinhaelter J. and Kopecký V., J. Plas. Phys. **10** (1973) 1-12.